DOI: 10.1002/chem.200902229

Kinetic Resolution of Aminoalkenes by Asymmetric Hydroamination: A Mechanistic Study

Alexander L. Reznichenko,[a] Frank Hampel,[b] and Kai C. Hultzsch*[a]

Abstract: The kinetic resolution of chiral aminoalkenes by hydroamination–cyclization was studied by using 3,3′-bis(triarylsilyl)-substituted binaphtholate rare-earth-metal complexes. The resolution of 1-arylaminopentenes proceeds with high efficiency and high *trans*-diastereoselectivity, whereas the resolution process of 1-alkylaminopentenes suffers from decreasing resolution efficiency with increasing steric demand of the aliphatic substituent. Kinetic studies of the matching and mismatching substrate–catalyst pair by using enantiopure substrates and either the (*R*)- or (*S*)-binaphtholate catalysts revealed that the difference in resolution efficiency stems from a shift of the Curtin–Hammett pre-equilibrium. Although 1-arylaminopentenes favor the matching substrate–catalyst complex, preference for the mismatching substrate–catalyst complex for 1-alkylaminopentenes diminishes resolution efficiency. Nevertheless, the relative cyclization rate for the two diastereomeric substrate–catalyst complexes remains in a typical range of 7–10:1. Plausible attractive π interactions between the aryl substituent and either the metal center or the aromatic system of the bis(triarylsilyl)-substituted binaphtholate ligand may explain increased stability of the matching substrate–catalyst complex. Incidentally, the methoxymethyl (MOM)-substituted aminopentene **3g** also exhibited a strong preference for the matching substrate–catalyst complex, possibly due to the chelating nature of the MOM substituent. The proximity of the stereocenter to the amino group in the aminoalkene substrate was crucial to achieve good kinetic resolution efficiency. The more remote β-phenyl substituent in 2-phenylpent-4-en-1-amine (**5**) resulted in diminished discrimination of the substrate enantiomers with respect to the relative rate of cyclization of the two substrate–catalyst complexes and a Curtin–Hammett pre-equilibrium close to unity.

Keywords: asymmetric catalysis · hydroamination · kinetic resolution · reaction mechanisms · rare earths

Introduction

The importance of nitrogen-containing compounds in biological systems and industrially relevant basic and fine chemicals has sparked significant research efforts to develop efficient synthetic protocols.[1] One of the simplest approaches, hydroamination, has only found significant attention in recent years with the development of more efficient transition-metal-based catalyst systems.[2] The addition of amine N–H functionalities to unsaturated carbon–carbon bonds, either in an intermolecular (Scheme 1a) or intramolecular (Scheme 1b) fashion, generates amines in a waste-free, highly atom-economical manner starting from simple and inexpensive precursors.

In particular, the generation of new stereogenic centers constitutes an attractive application of the hydroamination process, but the development of chiral catalysts for the asymmetric hydroamination of alkenes (AHA) has remained challenging.[3,4]

[a] A. L. Reznichenko, Prof. Dr. K. C. Hultzsch
Department of Chemistry and Chemical Biology
Rutgers, The State University of New Jersey
610 Taylor Road, Piscataway, NJ 08854-8087 (USA)
Fax: (+1) 732-445-5312
E-mail: hultzsch@rci.rutgers.edu

[b] Dr. F. Hampel
Institut für Organische Chemie
Friedrich-Alexander Universität Erlangen-Nürnberg
Henkestr. 42, 91054 Erlangen (Germany)

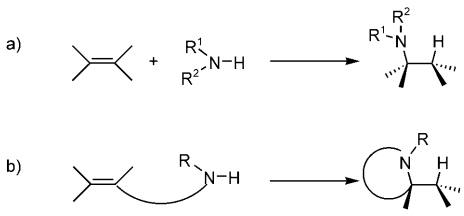

Scheme 1. Inter- (a) and intramolecular (b) hydroamination of alkenes.

 © 2009 Wiley-VCH Verlag GmbH & Co. KGaA, Weinheim

Among the various catalyst systems developed over the past two decades,[2,5] rare-earth-metal complexes are among the most active and widely applicable catalysts.[2l,6–8]

In recent years, limitations in the enantioselectivities obtained with chiral lanthanocene-based hydroamination catalysts[3,9] sparked the development of novel, chiral, non-metallocene-based rare-earth-metal hydroamination catalysts.[10–13] Our investigations have focused on the development of chiral biphenolate and binaphtholate rare-earth-metal hydroamination catalysts.[11] In particular, complexes based on sterically demanding 3,3′-bis(triarylsilyl)-substituted binaphtholate ligands[11c,d] have proven to be highly active and enantioselective, achieving up to 95% enantiomeric excess (*ee*) in hydroamination–cyclization of aminoalkenes. Furthermore, these complexes were also efficient in the catalytic kinetic resolution of chiral aminoalkenes by hydroamination–cyclization (Scheme 2).[14,15]

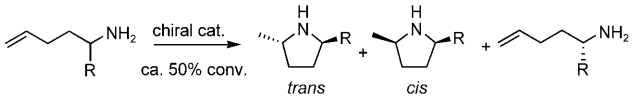

Scheme 2. Kinetic resolution by hydroamination–cyclization.

Kinetic resolution of chiral α-substituted aminoalkenes containing aryl substituents proceeded smoothly with high diastereoselectivity (*trans*/*cis* up to 50:1) and high resolution factors (*f* up to 19). Unfortunately, kinetic resolution of chiral α-substituted aminoalkenes containing aliphatic substituents proceeded with deteriorating efficiency, but increasing *trans*/*cis* diastereoselectivity, with increasing steric demand of the alkyl substituent. Herein, we disclose results from a detailed kinetic study of this kinetic resolution process, which sheds some light on the mechanism of this catalytic asymmetric hydroamination and the mode of operation of the chiral binaphtholate catalysts.

Results and Discussion

During our previous studies, we have demonstrated that chiral rare-earth-metal binaphtholate complexes **1**–Ln and **2**–Ln (Ln = Sc, Y, Lu) are active in both hydroamination–cyclization and kinetic resolution of 1-substituted aminopentenes.[11c,d]

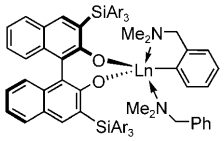

(*R*)-**1**-Ln: Ar = Ph
(*R*)-**2**-Ln: Ar = 3,5-$Me_2C_6H_3$
Ln = Sc, Y, Lu

In an extension of our previous study we surveyed a broader set of α-substituted aminoalkenes with six different binaphtholate rare-earth-metal complexes **1**–Ln and **2**–Ln (Table 1). As noted previously, the highest resolution factors were observed for the α-aryl-substituted aminoalkenes **3a–c**, with **1**–Lu being most efficient for **3a**.[11d] In contrast to general trends in (nonkinetic-resolution-type) asymmetric hydroamination reactions, the efficiency in kinetic resolution often increases with the ionic radius size of the rare-earth metal. For example, the triphenylsilyl-substituted binaphtholate yttrium complex **1**–Y was superior for the 4-methoxyphenyl-substituted aminopentene **3b** (Table 1, entry 5), whereas the sterically more congested tris(3,5-xylyl)silyl-substituted binaphtholate yttrium complex **2**–Y was most efficient for the electron-withdrawing 4-chlorophenyl-substituted aminopentene **3c** (Table 1, entry 14).

For α-alkyl-substituted aminoalkenes, high selectivities are only observed for the sterically least demanding sub-

Table 1. Kinetic resolution parameters of α-substituted aminopentenes[a]

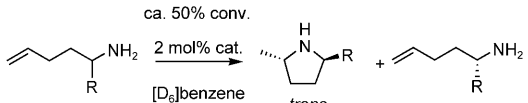

3a: R = Ph
3b: R = 4-$MeOC_6H_4$
3c: R = 4-ClC_6H_4
3d: R = CH_2Ph
3e: R = Me
3f: R = Cy
3g: R = CH_2OMe

Entry	Subst.	Cat.	*t* [h]	*T* [°C]	Conv. [%]	*ee* [%][b]	*f*
1	**3a**	**1**–Y	95	22	50	74	15[c]
2	**3a**	**1**–Lu	15	40	52	83	19[c]
3	**3a**	**2**–Y	18	40	52	63	7[c]
4	**3a**	**2**–Lu	40	22	52	59	6[c]
5	**3b**	**1**–Y	8	40	50	78	19[c]
6	**3b**	**1**–Lu	26	40	47	70	18
7	**3b**	**1**–Sc	35	50	55	69	7
8	**3b**	**2**–Y	14	40	34	40	12
9	**3b**	**2**–Lu	24	40	52	70	11
10	**3b**	**2**–Sc	22	50	51	54	6
11	**3c**	**1**–Y	18	40	50	71	12[c]
12	**3c**	**1**–Lu	17	40	55	77	10
13	**3c**	**1**–Sc	22	50	60	81	8
14	**3c**	**2**–Y	10	40	51	80	19
15	**3c**	**2**–Lu	21	40	50	68	11
16	**3c**	**2**–Sc	24	50	49	68	12
17	**3d**	**1**–Y	9	22	50	42	3.6[c]
18	**3d**	**1**–Lu	26	22	50	32	2.6
19	**3d**	**1**–Sc	40	40	64	60	3.5
20	**3d**	**2**–Y	27	22	52	38	2.9[c]
21	**3d**	**2**–Lu	13	22	70	42	2.0
22	**3d**	**2**–Sc	33	40	55	47	3.5
23	**3e**	**1**–Y	25.5	22	53	72	9.5[c]
24	**3e**	**1**–Lu	42	22	55	73	8.4[c]
25	**3e**	**1**–Sc	94	40	51	73	12[c]
26	**3e**	**2**–Y	26	22	52	80	16[c]
27	**3e**	**2**–Lu	24.5	22	51	75	14[c]
28	**3e**	**2**–Sc	94	40	50	73	14[c]
29	**3f**	**1**–Y	8	22	56	49	3.5
30	**3f**	**1**–Lu	23	22	47	51	6.0
31	**3f**	**1**–Sc	34	40	75	67	2.9
32	**3f**	**2**–Y	46	22	59	54	3.6
33	**3f**	**2**–Lu	47	22	46	44	4.7
34	**3f**	**2**–Sc	49	40	47	32	2.8
35	**3g**	**1**–Y	85	40	50	33	2.7
36	**3g**	**1**–Lu	120	40	59	9	1.2
37	**3g**	**2**–Y	180	40	45	20	2.0
38	**3g**	**2**–Lu	94	40	56	9	1.2

[a] Reaction conditions: 2 mol% cat., [D_6]benzene, Ar atm, 0.5–1 M substrate (subst.). Conv. = conversion. [b] *ee* value of recovered **3**. [c] Data from ref. [11d].

 © 2009 Wiley-VCH Verlag GmbH & Co. KGaA, Weinheim

strate **3e** by using the sterically more demanding tris(3,5-xylyl)silyl-substituted catalyst **2** in general and, in particular, the yttrium complex **2**–Y. Sterically more demanding α-alkyl substrates, such as the benzyl-substituted **3d** and the cyclohexyl-substituted **3f**, exhibit significantly diminished resolution factors. Both scandium and yttrium complexes show slightly higher kinetic resolution efficiency for **3d**, whereas the opposite observation (highest selectivity for **1**–Lu, Table 1, entry 30) is true for **3f**. The cyclization of the methoxymethyl (MOM)-substituted aminoalkene **3g** is significantly retarded, clearly due to the chelating nature of the pending ether functionality. Contrary to our expectations, the chelating donor group did not improve the kinetic resolution efficiency, with essentially no kinetic discrimination of the two substrate enantiomers for lutetium catalysts and only slightly better efficiencies for yttrium catalysts. Again, the highest selectivity was observed for **1**–Y (Table 1, entry 35).

According to the general model for the kinetic resolution of racemic aminoalkenes by catalytic hydroamination (Scheme 3),[11d] the total amount of the catalyst [Ln] is distributed between two substrate–catalyst complexes [cat.-*S*] and [cat.-*R*] [Eq. (1)], which readily interconvert with an equilibrium constant, K^{dias}, determined by Equation (2). Each of the complexes reacts with a corresponding rate constant (k_R and k_S) to give the corresponding hydroamination products. Previous NMR spectroscopic investigations of **1**–Y and **2**–Y have revealed that the rate of interconversion between the two diastereomeric substrate–catalyst complexes is rapid, even at low temperatures, and significantly higher than both rates of cyclization.[11d]

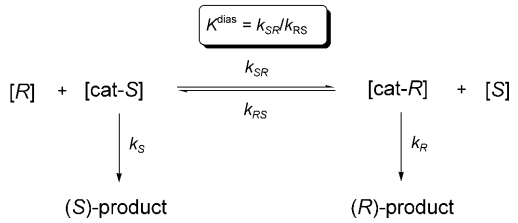

Scheme 3. General model for catalytic kinetic resolution.

$$[\mathrm{Ln}] = [\text{cat.-}S] + [\text{cat.-}R] \quad (1)$$

$$K^{\mathrm{dias}} = \frac{k_{SR}}{k_{RS}} = \frac{[\text{cat.} - R][S]}{[\text{cat.} - S][R]} \quad (2)$$

The resolution factor f depends on three independent parameters: the equilibrium constant (K^{dias}) and the cyclization rate constants of both substrate–catalyst complexes [Eq. (3)],[16] which may be determined independently.

$$f = K^{\mathrm{dias}}\frac{k_R}{k_S} \quad (3)$$

For pseudo-first-order reactions [Eqs. (4) and (5)], the resolution factor can be expressed as a function of the conversion (C) and the *ee* value of the recovered substrate [(Eq. (6)]:

$$-\frac{d[R]}{dt} = k_R[\text{cat.} - R] \quad (4)$$

$$-\frac{d[S]}{dt} = k_S[\text{cat.} - S] \quad (5)$$

$$f = \frac{\ln([R]/[R]_0)}{\ln([S]/[S]_0)} = \frac{\ln[(1-C)(1+ee)]}{\ln[(1-C)(1-ee)]} \quad (6)$$

A plot of $\ln[(1-C)(1+ee)]$ versus $\ln[(1-C)(1-ee)]$ provides the resolution factor f (Figure 1), while kinetic measurements obtained by using an enantiopure substrate and either the (*R*)- or (*S*)-catalyst gives access to the zero-order reaction rate constants k_R and k_S for the matching (Figure 2a) and mismatching (Figure 2b) substrate–catalyst combination. Enantiopure substrates were obtained either through large-scale kinetic resolution (**3a**–**3f**, Table 2) by using the best resolution catalysts for each particular substrate or by fractional crystallization of the ammonium salt with (*R*)-(−)-mandelic acid (**3g**).[17] The kinetic data and resolution parameters obtained for substrates **3a**–**3g** by using (*R*)-**1**–Y and (*S*)-**1**–Y are summarized in Table 3.

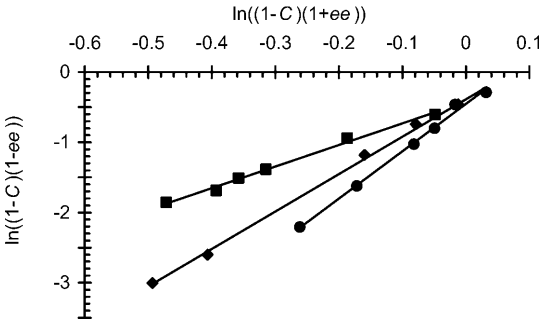

Figure 1. Plot of $\ln[(1-C)(1+ee)]$ versus $\ln[(1-C)(1-ee)]$ for the kinetic resolution of **3e** by using (*R*)-**1**–Y as a catalyst at various temperatures (● = 30 °C, ◆ = 40 °C, ■ = 50 °C).

In agreement with our previous findings for the phenyl-substituted substrate **3a**,[11d] the aryl-substituted substrates **3b** and **3c** both exhibit an equilibrium constant K^{dias} in favor of the matching substrate–catalyst complex ($K^{dias} > 1$). Thus, K^{dias} and the k_R/k_S ratio both favor the resolution process. Also, cyclization of **3b** and **3c** proceeded with the same high diastereoselectivities as that for **3a**.

The cyclization of the *N*-deuterated aminoalkene [D_2]**3a** proceeded with a significant primary kinetic isotope effect (KIE, $k_H/k_D = 3.8$ at 50 °C and 5.4 at 60 °C), which is in agreement with previous findings on the hydroamination–cyclization of achiral aminopentenes.[6a,11d] Although no N–H bond breaking is involved in the rate-determining olefin-insertion step according to the generally accepted mechanism for the hydroamination–cyclization of aminoalkenes,[2l,6a] it has been proposed that partial proton trans-

 © 2009 Wiley-VCH Verlag GmbH & Co. KGaA, Weinheim

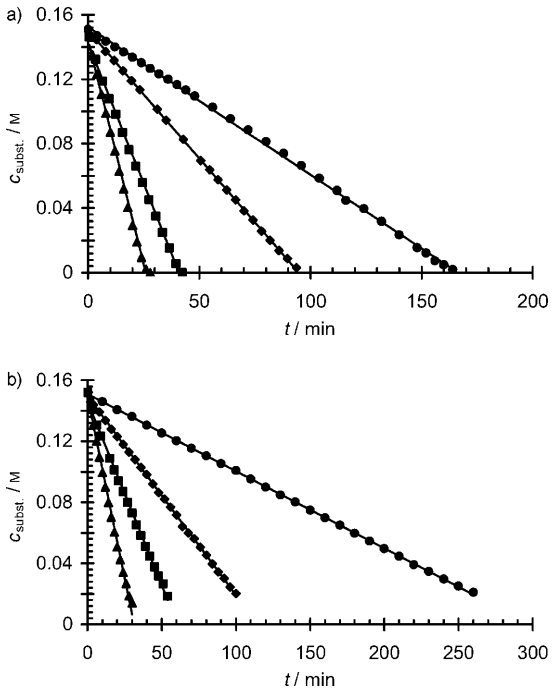

Figure 2. Time dependence of substrate consumption in the hydroamination–cyclization of (*R*)-**3e** with a) (*S*)-**1**–Y (matching pair;[16] [cat.]= 0.00228 M) and b) (*R*)-**1**–Y (mismatching pair;[16] [cat.]=0.00833 M) in [D_6]benzene; [**3e**]$_0$=0.152 M (●=30 °C, ◆=40 °C, ■=50 °C, ▲=60 °C).

Table 2. Preparation of highly enantioenriched α-substituted aminopentenes by kinetic resolution.

Subst.	Cat.	T [°C]	f	Conv. [%]	Yield (*ee*) [%][a]
[D_2]**3a**	(*R*)-**1**–Lu	40	19	61	34 (98)
3b	(*R*)-**1**–Lu	40	18	60	36 (98)
3c	(*R*)-**2**–Y	40	19	61	30 (97)
3d	(*R*)-**1**	25	5	83	12 (>98)
3e	(*R*)-**2**–Y	25	15	64	30 (97)
3f	(*R*)-**1**–Lu	25	6	84	9 (98)

[a] Yield and *ee* value of recovered **3**.

fer from a coordinated amine may stabilize the four-membered-ring olefin-insertion transition state.[6a] Despite this pronounced KIE, both reaction channels are affected to a similar extent and the resulting resolution parameters seem to be similar to those of the nondeuterated substrate **3a**.

Compared with the aryl-substituted aminoalkenes **3a–3c**, the alkyl- and benzyl-substituted aminopentenes **3d–3f** behaved quite differently. Here, the Curtin–Hammett preequilibrium favored the mismatching substrate–catalyst complex ($K^{dias}<1$), thus, effectively reducing the efficiency of the kinetic resolution process. A notable exception is the MOM-substituted substrate **3g**, which displayed a preference for the matching substrate–catalyst complex, possibly as a result of the coordinating donor substituent. Diastereoselectivities were lower for substrates **3e–3g** than for **3a–3d** and the mismatching substrate–catalyst combination exhibited significantly reduced diastereoselectivities. Interestingly, the benzyl-substituted aminoalkene **3d** combines properties of both substrate families, that is, a Curtin–Hammett pre-

Table 3. Kinetic resolution parameters of α-substituted aminopentenes determined with **1**–Y.

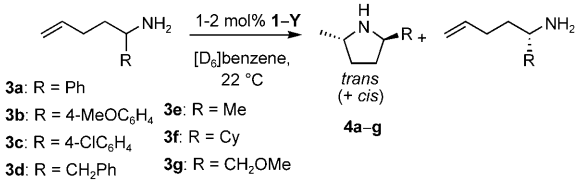

	Subst.	T [°C]	f	k_{fast} [10^{-3} s^{-1}][a]	k_{fast}/k_{slow}[b]	K^{dias}	*trans*/*cis* fast (slow)[c]
1	**3a**	50	12.8	5.45	6.6	1.9	>50:1 (9.2:1)[d]
2	**3a**	60	11.5	11.3	7.1	1.6	>50:1 (8.8:1)[d]
3	[D_2]**3a**	50	11.0	1.42	5.3	2.1	>50:1 (15:1)
4	[D_2]**3a**	60	9.1	2.10	4.9	1.9	>50:1 (15:1)
5	**3b**	40	18.1	0.81	9.5	1.9	>50:1 (>50:1)
6	**3c**	40	13.2	4.5	4.2	3.1	>50:1 (>50:1)
7	**3d**	30	2.6	2.5	9.6	0.27	>30:1 (>30:1)
8	**3e**	30	6.4	8.5	7.6	0.84	>30:1 (2.8:1)
9	**3e**	40	5.2	14.0	7.1	0.73	>30:1 (2.2:1)
10	**3e**	50	4.1	30.4	7.0	0.59	>30:1 (2.1:1)
11	**3f**	30	2.7	8.5	8.5	0.32	9:1 (1.4:1)
12	**3g**	50	4.1	2.2	3.2	1.28	6:1 (2:1)
13	**3g**	60	6.6	5.1	3.4	1.93	5:1 (1.8:1)

[a] $k_{fast}=k_R$ for **3a–3d**, **3f**, and **3g**; $k_{fast}=k_S$ for **3e**. [b] $k_{fast}/k_{slow}=k_R/k_S$ for **3a–3d**, **3f**, and **3g**; $k_{fast}/k_{slow}=k_S/k_R$ for **3e**. [c] Determined by integration of C*H*N proton signals of pyrrolidines in the ^{1}H NMR spectra after full conversion. [d] Kinetic data from ref. [11d].

equilibrium in favor of the mismatching substrate–catalyst complex, while achieving high *trans*/*cis*-diastereoselectivities.

Although the equilibrium constant is strongly affected by the α-substituent, the relative reaction rate k_R/k_S remains in the range of 7–10 for all of the substrates, except **3c** and **3g**.

The activation parameters for the matching ($\Delta H^{\ddagger}=(47.3\pm3.5)$ kJ mol^{-1}, $\Delta S^{\ddagger}=(-128\pm11)$ J K^{-1} mol^{-1}) and mismatching ($\Delta H^{\ddagger}=(54.9\pm3.1)$ kJ mol^{-1}, $\Delta S^{\ddagger}=(-121\pm9)$ J K^{-1} mol^{-1}) substrate–catalyst combination for the cyclization of **3e** were obtained from the Eyring plot for k_{fast} and k_{slow} (Figure 3). The data compare well with the parameters obtained previously for **3a** (matching: $\Delta H^{\ddagger}=(52.2\pm2.8)$ kJ mol^{-1}, $\Delta S^{\ddagger}=(-127\pm8)$ J K^{-1} mol^{-1}; mismatching: $\Delta H^{\ddagger}=(57.7\pm1.3)$ kJ mol^{-1}, $\Delta S^{\ddagger}=(-126\pm$

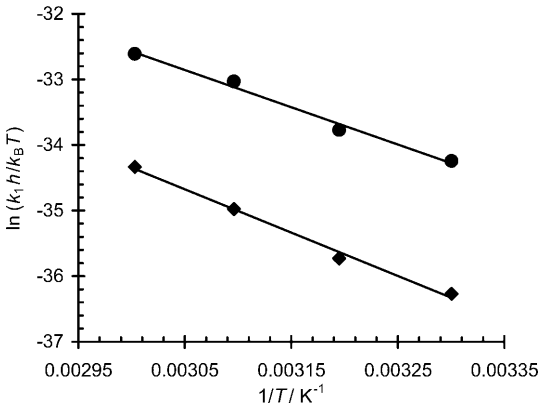

Figure 3. Eyring plot for the hydroamination–cyclization of (*R*)-**3e** by using (*S*)-**1**–Y (●, matching, $y=-5691.3x-15.496$, $R^2=0.989$) and (*R*)-**1**–Y (◆, mismatching, $y=-6608.9x-14.518$, $R^2=0.9939$).

 © 2009 Wiley-VCH Verlag GmbH & Co. KGaA, Weinheim

4) $J K^{-1} mol^{-1}$).[11d] The negative activation entropy is a strong indicator of a highly organized transition state.[6a,11d]

X-ray crystallographic and optical rotational evidence show that the (*R*)-binaphtholate catalysts react faster with (*R*)-**3a**–**3d** and (*S*)-**3e**. A comparison of the ^{19}F NMR spectra of the Mosher amides also indicates that (*R*)-**3f** and (*R*)-**3g** are the matching substrates for these catalysts. A stereomodel for the binaphtholate rare-earth-metal-catalyzed kinetic resolution of α-substituted aminoalkenes by intramolecular hydroamination in agreement with these findings has been proposed (Scheme 4).[11d] According to this model, the

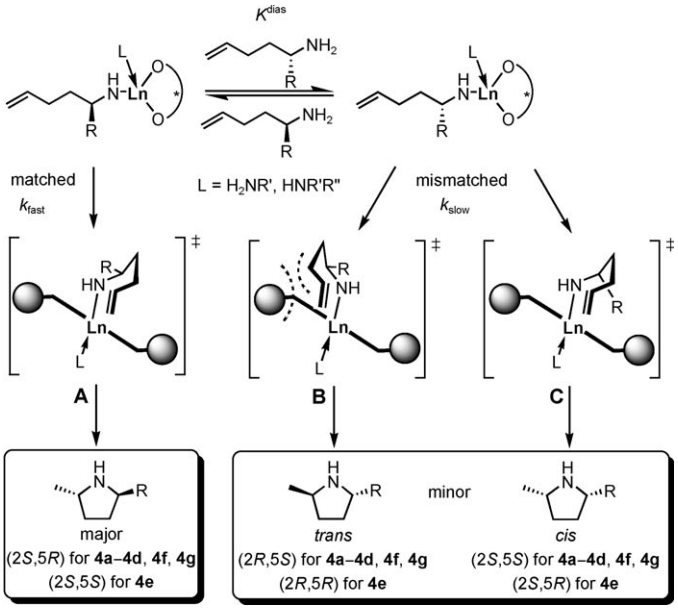

Scheme 4. Stereomodel for kinetic resolution of α-substituted aminopentenes. For the matching substrate only the pathway leading to the preferred *trans* isomer is shown.

rare-earth-metal amide preferentially approaches the alkene moiety from the *re* face (Scheme 4, **A**), whereas the approach from the *si* face of the alkene is hampered due to unfavorable repulsive interactions between the substrate alkyl chain and the sterically demanding triarylsilyl substituent of the (*R*)-binaphtholate ligand (Scheme 4, **B**). Each of the two diastereomeric substrate–catalyst complexes has two possible cyclization pathways.

The high *trans* diastereoselectivities observed for aryl-substituted aminopentenes suggests that these substrates preferably cyclize through a transition state with an equatorial orientation of the aryl substituent in both substrate–catalyst complexes. This may be explained either by a potential coordinative interaction of the phenyl ring with the metal[18] or a π interaction with a naphthyl ring of the binaphtholate ligand, thus providing additional stabilization to the equatorial complex. Furthermore, this weak attractive interaction of the aryl substituent in **3a**–**3c** may explain the slight preference for the matching substrate–catalyst complex over the mismatching complex ($K^{dias} > 1$) and similar donor–metal interactions can be proposed for the methyl ether substituted **3g**. Interestingly, the equilibrium constant K^{dias} for **3g** increases with increasing temperature, whereas the aryl-substituted **3a** displays the opposite behavior.

The decreased *trans*/*cis* diastereoselectivity observed for the mismatched substrate–catalyst combination for **3a**, **3e**, and **3f** can be rationalized with an alternative approach of the metal–amide bond to the *re* face of the alkene moiety, in which the α substituent rests in an axial position (Scheme 4, **C**). Interestingly, substrates **3b**–**3d** exhibit the same high level of *trans* diastereoselectivity, suggesting that unfavorable steric interactions of these larger, more extended α substituents with the triarylsilyl substituent of the binaphtholate ligand preclude reaction pathway **C** becoming an alternative to pathway **B**.

To investigate the general influence of the position of the aryl substituent in the substrate on the resolution process, we investigated the kinetic resolution of the β-phenyl-substituted aminopentene **5** (Table 4).

Table 4. Kinetic resolution of **5** ([subst.]$_0$ = 2.0 M) by using 2 mol% binaphtholate catalysts **1**–Ln and **2**–Ln at 25 °C.

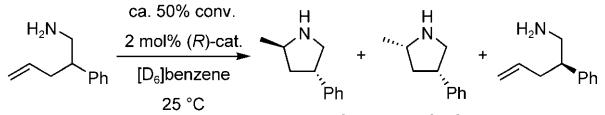

Cat.	Conv. [%][a]	*trans*/*cis*[b]	*ee* [%][c]	*f*
(*R*)-**1**–Y	53	1:1.3	17	1.6
(*R*)-**1**–Lu	51	1:1.3	26	2.1
(*R*)-**1**–Sc	54	1:1.3	34	2.5
(*R*)-**2**–Y	47	1:1.2	17	1.8
(*R*)-**2**–Lu	55	1:1.2	31	2.2
(*R*)-**2**–Sc	50	1:1.2	11	1.4

[a] Determined by ^1H NMR spectroscopy using ferrocene as an internal standard. [b] Determined by ^1H NMR spectroscopy. [c] *ee* value of recovered **5**, determined by ^{19}F NMR spectroscopy of the corresponding Mosher amide.

Although the preparative-scale kinetic resolution of **5** could not be achieved due to the low resolution factors, we succeeded in isolating enantiopure (*S*)-**5** after repeated recrystallization of the corresponding (*R*)-mandelate. The absolute configuration was established by X-ray crystallographic analysis of the corresponding Mosher amide.[19] ^{19}F NMR spectroscopic analysis of the Mosher amide of **5**, recovered from the kinetic resolution reaction, carried out by using complexes (*R*)-**1** and (*R*)-**2**, was thus identified to be the (*R*)-enantiomer, indicating that (*S*)-**5** reacts faster with the (*R*)-binaphtholate catalysts. With (*S*)-**5** in hand, we began to study the kinetics and diastereoselectivity of the matching and mismatching substrate–catalyst pairs (Table 5) by using **1**–Y as the catalyst.

Table 5 illustrates that, in contrast to **3a–3g**, kinetic resolution of **5** proceeded with very low reaction rate difference, k_{fast}/k_{slow}, between the matching and mismatching substrate–catalyst pair. Furthermore, with $K^{dias} \approx 0.9$, the mismatching substrate–catalyst complex is slightly favored in the Curtin–Hammett pre-equilibrium. Overall, the more remote place-

 © 2009 Wiley-VCH Verlag GmbH & Co. KGaA, Weinheim

Table 5. Kinetic resolution parameters for **5** by using **1–**Y.[a]

T [°C]	f	k_{fast} [10^{-3} s^{-1}][a]	k_{fast}/k_{slow}	K^{dias}	*trans*/*cis* matching (mismatching)
30	1.5	0.58	1.64	0.92	1:1.3 (6:1)
40	1.5	1.32	1.73	0.87	1:1.4 (7:1)
50	1.4	3.00	1.48	0.95	1:1.4 (7:1)

[a] The rates for the matching and mismatching substrate–catalyst combination were determined with (*S*)-**5** by using either (*R*)-**1–**Y (matching combination) or (*S*)-**1–**Y (mismatching combination).

ment of the phenyl substituent in the β position to the amino group significantly diminishes its influence on the kinetic resolution. However, it is noteworthy that the *trans*/*cis* diastereomeric ratio shifts dramatically going from the matching to the mismatching substrate–catalyst pair. The matching substrate–catalyst combination indicates a slight preference for formation of the *cis*-pyrrolidine diastereomer, which is in agreement with a preferred equatorial orientation of the phenyl substituent in the approach of the metal amide to the *re* face of the alkene moiety (Scheme 5, **A**).

The strong preference for the *trans*-pyrrolidine product in the case of the mismatching substrate–catalyst combination may be explained by the presence of an additional steric interaction between the equatorial phenyl substituent and the triarylsilyl-substituted binaphtholate ligand in the approach of the metal amide bond to the *si* face of the alkene leading to the *cis*-pyrrolidine (Scheme 5, **C**). Alternatively, the approach to the *re* face (Scheme 5, **D**) leading to the *trans*-pyrrolidine puts the phenyl substituent in an axial position without disadvantageous steric interactions with the binaphtholate ligand. Thus, in contrast to **3a–3c**, there is no tendency to keep the phenyl ring in an equatorial position.

We then directed our attention to the kinetic resolution of 3-phenylpent-4-en-1-amine (**7**), which features a phenyl substituent in the γ position relative to the amino group and in the allylic position relative to the alkene moiety. We anticipated that the closer proximity to the alkene might increase the influence on the outcome of the kinetic resolution. Unfortunately, the kinetic resolution of **7** led to partial double bond isomerization. Nevertheless, enantioenriched (*S*)-**7** was recovered from the reaction mixture at approximately 50% conversion (Table 6).

Table 6. Attempted NMR-scale kinetic resolution of **7** at 30 °C.

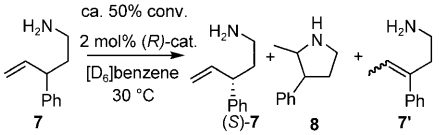

Cat.	Conv. [%]	**8**:**7′**	*ee* [%][a]	f
(*R*)-**1**–Y	47	7:1	39	3.7
(*R*)-**2**–Y	51	6:1	65	8.2

[a] *ee* value of recovered **7**, determined by chiral phase HPLC of the 2-naphthoyl amide of **7** recovered from the reaction mixture.

In our previous study, we reported the kinetic resolution of hept-6-en-2-amine with a moderate resolution factor of 3.3 using (*R*)-**2–**Y at 80 °C.[11d] We hoped that better resolution factors may be achieved in the kinetic resolution of the aryl-substituted aminohexene **9**, but, unfortunately, the resolution factor was limited to less than three for this substrate (Table 7), which was insufficient for a preparative-scale kinetic resolution.

Conclusion

Kinetic investigations into the kinetic resolution of chiral aminopentenes with sterically hindered triarylsilyl-substituted binaphtholate rare-earth-metal complexes **1** and **2** were carried out. These indicated that substrates with substituents in the α position that can interact with the metal center (or the aromatic ring system of the binaphtholate ligands), for example, through π–arene coordination or an ether donor group, favor the matching substrate–catalyst complex, resulting in good efficiencies in the kinetic resolution process. Simple aliphatic substituents, on the other hand, favor the mismatching substrate–catalyst complex, which significantly diminishes the efficiency in the kinetic resolution.

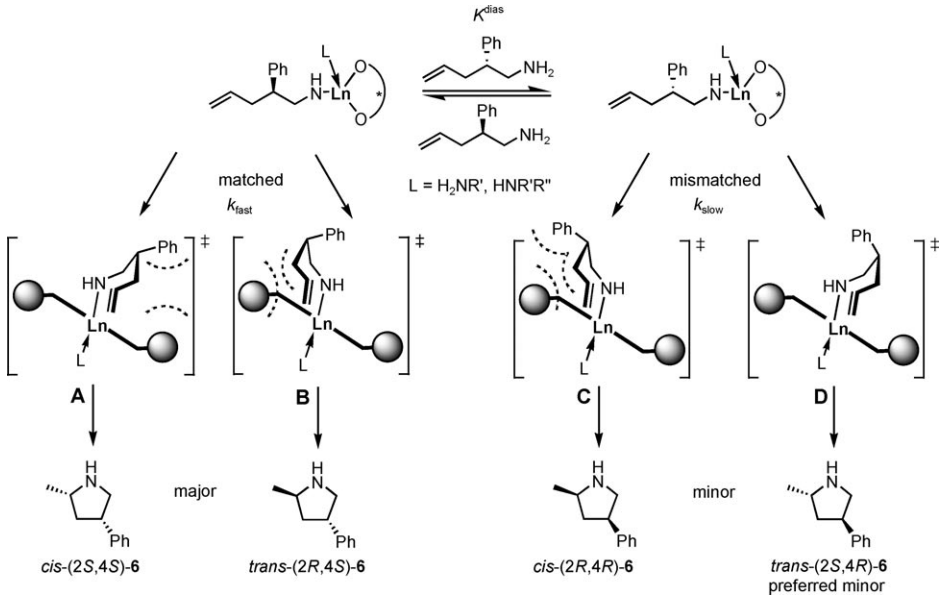

Scheme 5. Proposed transition states in the kinetic resolution of **5**.

 © 2009 Wiley-VCH Verlag GmbH & Co. KGaA, Weinheim

Table 7. Kinetic resolution of aminohexene **9** ([subst.]$_0$ = 2.0 M) by using binaphtholate catalysts (*R*)-**1** and (*R*)-**2** at 80 °C.

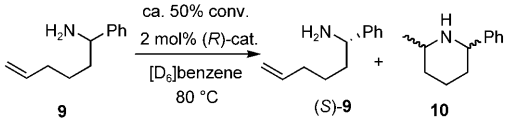

Cat.	Conv. [%][a]	*trans*/*cis*[b]	*ee* [%][c]	*f*
(*R*)-**1**–Y	45	1:3	11	1.5
(*R*)-**1**–Lu	51	1:6	26	2.1
(*R*)-**1**–Sc	47	1:7	18	1.5
(*R*)-**2**–Y	72	1:2.5	11	1.3
(*R*)-**2**–Lu	55	1:5	31	2.2
(*R*)-**2**–Sc	60	1:4	47	2.9

[a] Determined by ^{1}H NMR spectroscopy based on an internal standard. [b] Determined by ^{1}H NMR spectroscopy. [c] *ee* of recovered **9** determined by ^{19}F NMR spectroscopy of the corresponding Mosher amide.

Experimental Section

General: All operations were performed under an inert atmosphere of nitrogen or argon by using standard Schlenk-line or glove box techniques. Solvents and reagents were purified as stated previously.[11] Complexes **1**–Ln and **2**–Ln (Ln = Sc, Y, Lu),[11d] substrates **3a–3d**,[11d] **3e**,[7i] **5**,[7i] and, **7**[20] were prepared according to previously described procedures. (*R*)-(+)-α-Methoxy-α-trifluoromethylphenylacetic acid was transformed to its acid chloride by using oxalyl chloride/DMF in hexanes.[21] Enantiomeric excess for **3a–3g** was measured by ^{19}F NMR spectroscopy of the corresponding Mosher amides as reported previously.[11d] The enantiomeric excess for **7** was measured by chiral phase HPLC of the corresponding 2-naphthoyl amide on a Chiralcel OD column, eluent hexane/isopropyl alcohol = 90:10, flow rate 1 mL min^{-1}, retention times 39.0 min (major isomer obtained from the *R* catalyst); 41.2 min (minor isomer). The absolute configuration of enantioenriched **7** was established by comparison of the optical rotation sign of the *N*-benzoyl derivative with the literature data.[22]

[D$_2$]-1-Phenylpent-4-en-1-amine ([D$_2$]3a): A mixture of **3a** (1.60 g, 9.9 mmol), hexanes (5 mL), and D_2O (2 mL) was stirred in a sealed flask at 60 °C overnight. After cooling to room temperature, the aqueous layer was separated and discarded. The procedure was repeated twice with fresh aliquots of D_2O (2 mL). The organic layer was dried over molecular sieves and the solvent was removed in vacuo. The residue was distilled twice from CaH_2 at reduced pressure to give [D$_2$]**3a** (1.20 g, 74 %) as a colorless liquid (b.p. 120 °C, 1 mmHg) with > 95 % of isotopic substitution according to ^{1}H NMR spectroscopy. Mosher adduct: ^{19}F NMR ([D$_6$]benzene, 60 °C): $\delta = -69.35$ (*R*), −69.47 ppm (*S*).

1-Cyclohexylpent-4-en-1-amine (3f): Copper(I) iodide (200 mg, 1.05 mmol) was added to a solution of cyclohexanecarboxylic acid chloride (5.84 g, 39.8 mmol) in THF (100 mL). The resulting suspension was cooled to −30 °C and a solution of but-3-enemagnesium bromide prepared from 4-bromobut-1-ene (5.40 g, 40.0 mmol) and magnesium turnings (0.96 g, 39.5 mmol) in THF (100 mL) was added dropwise over 1 h, while the temperature was maintained below −20 °C. The mixture was stirred at the same temperature for 2 h and was then allowed to warm to room temperature. The solvent was removed in vacuo, the residue was dissolved in CH_2Cl_2 (70 mL) and 1 M aqueous HCl (50 mL). The organic layer was separated, filtered to remove precipitated copper salts, washed with 10 % aqueous $NaHCO_3$, and dried over Na_2SO_4. The solvent was removed by rotary evaporation and the residue was dissolved in absolute MeOH. Ammonium acetate (15 g, 200 mmol) and $NaBH_3CN$ (1.0 g, 15 mmol) were added in one portion at room temperature. The mixture was stirred at room temperature for 1 d. Concentrated HCl was added carefully until pH < 2 was reached and the solvent was removed in vacuo. The residue was dissolved in water (50 mL) and extracted once with diethyl ether (20 mL). The aqueous solution was brought to pH > 12 with solid KOH and extracted with diethyl ether (3 × 20 mL). The combined extracts were dried over KOH and the solvent was evaporated in vacuo. The residue was treated with finely powdered CaH_2 for 2 h and was then distilled twice from CaH_2 at reduced pressure to give **3f** as a colorless liquid (4.20 g, 62 %). B.p. 120 °C at 1 mmHg; ^{1}H NMR (400 MHz, $CDCl_3$): $\delta = 5.85$–5.75 (m, 1H; =CH), 5.01–4.87 (m, 2H; $=CH_2$), 2.50–2.43 (m, 1H; $CHNH_2$), 2.22–2.02 (m, 2H; CH_2), 1.72–1.51 (m, 6H; CH_2), 1.28–0.83 ppm (m, 9H; CH_2); ^{13}C{^{1}H} NMR (75.5 MHz, $CDCl_3$): $\delta = 138.8$ (=CH), 114.3 ($=CH_2$), 55.5, 43.9, 34.0, 30.8, 29.6, 27.8, 26.6, 26.5, 26.4 ppm; HRMS *m*/*z*: $[M]^+$ calcd for $C_{11}H_{22}N$: 168.1752 $[M-H]^+$; found: 168.1747; Mosher adduct ^{19}F NMR ($CDCl_3$, 25 °C): $\delta = -69.08$ (*R*), −69.25 ppm (*S*).

1-(Methoxymethyl)pent-4-enylamine (3g): Methoxyacetonitrile (7.11 g 0.10 mol) was added dropwise over 15 min at RT to a solution of but-3-enemagnesium bromide prepared from 4-bromobut-1-ene (13.5 g, 0.10 mol) and magnesium turnings (2.43 g, 0.10 mol) in THF (100 mL). The dark-red reaction mixture was stirred at reflux for 2 h. The mixture was then cooled and quenched with a saturated solution of aqueous ammonium chloride (100 mL). The product was extracted with diethyl ether (2 × 70 mL). The combined organic layers were washed with water, brine, and dried over Na_2SO_4. The solvent was evaporated in vacuo and the residue was dissolved in MeOH (200 mL). Ammonium acetate (61 g, 0.80 mol) and $NaBH_3CN$ (3.76 g, 60 mmol) were added in one portion at room temperature. The mixture was stirred at room temperature for 1 d. Concentrated HCl was added carefully until pH < 2 was reached and the solvent was removed in vacuo. The residue was dissolved in water (15 mL) and extracted with diethyl ether (20 mL). The aqueous solution was brought to pH > 12 with solid KOH and extracted with diethyl ether (3 × 20 mL). The combined extracts were dried over KOH and the solvent was evaporated in vacuo. The residue was treated with finely powdered calcium hydride for 2 h and was then distilled twice from CaH_2 at reduced pressure to give **3g** as a colorless liquid (4.50 g, 35 %). B.p. 95–104 °C at 200 mmHg; ^{1}H NMR (300 MHz, $CDCl_3$): $\delta = 5.86$–5.76 (m, 1H; =CH), 5.04–4.91 (m, 2H; $=CH_2$), 3.34–3.30 (m, 4H, CH_3; OCH_2), 3.16–3.11 (m, 1H; OCH_2) 2.96–2.92 (m, 1H; CHN), 2.20–2.02 (m, 2H; CH_2), 1.50–1.42 (m, 1H; CH_2), 1.39–1.30 (m, 1H; CH_2), 1.25 ppm (brs, 2H; NH_2); ^{13}C NMR (100 MHz, $CDCl_3$): $\delta = 138.4$ (=CH), 114.6 ($=CH_2$), 78.2, 58.9, 50.3, 33.4, 30.3 ppm; Mosher adduct ^{19}F NMR ([D$_6$]benzene, 70 °C): $\delta = -69.41$ (*S*), −69.48 ppm (*R*).

1-Phenyl-hex-5-en-1-amine (9): Copper(I) iodide (0.19 g, 1.0 mmol) was added to a solution of benzoyl chloride (4.20 g, 30 mmol) in THF (100 mL). The resulting suspension was cooled to −30 °C and a solution of pent-4-enemagnesium bromide prepared from 5-bromopent-1-ene (4.47 g, 30 mmol), and magnesium turnings (0.72 g, 30 mmol) in THF (50 mL) was added dropwise over 1 h, while the temperature was maintained below −20 °C. The mixture was stirred at the same temperature for 2 h and was then allowed to reach room temperature. The solvent was removed in vacuo and the residue was dissolved in dichloromethane (70 mL) and 1 M aqueous HCl (50 mL). The organic layer was separated, filtered to remove precipitated copper salts, washed with 10 % aqueous $NaHCO_3$, and dried over Na_2SO_4. The solvent was removed in vacuo and the residue was dissolved in absolute MeOH (100 mL). Ammonium acetate (15 g, 200 mmol) and $NaBH_3CN$ (2.0 g, 30 mmol) were added in one portion at room temperature. The mixture was stirred at room temperature for 1 d. Concentrated HCl was added carefully until pH < 2 was reached and the solvent was removed in vacuo. The residue was dissolved in water (50 mL) and extracted once with diethyl ether (20 mL). The aqueous solution was brought to pH > 12 with solid KOH and extracted with diethyl ether (3 × 20 mL). The combined extracts were dried over KOH and the solvent was evaporated in vacuo. The residue was treated with finely powdered calcium hydride for 2 h and was then distilled twice from CaH_2 at reduced pressure to yield **9** as a colorless liquid (3.70 g, 70 %). B.p. 95–99 °C at 0.5 mmHg; ^{1}H NMR (400 MHz, $CDCl_3$): $\delta = 7.36$–7.25 (m, 5H; aryl-H), 5.85–5.75 (m, 1H; =CH), 5.03–4.94 (m, 2H; $=CH_2$), 3.93 (t, ^3J(H,H) = 10.3 Hz, 1H; CH), 2.13–2.07 (m, 2H; CH_2), 1.76–1.69 (m, 2H; CH_2), 1.52–1.45 ppm (m, 4H; CH_2 and NH_2); ^{13}C{^{1}H} NMR (75.5 MHz, $CDCl_3$): $\delta = 146.7$ (aryl), 138.6 (=CH), 128.4, 126.9, 126.3 (aryl), 114.6 ($=CH_2$), 56.2, 39.1, 33.7, 25.8 ppm; Mosher adduct ^{19}F NMR ($CDCl_3$, 25 °C): $\delta = -69.29$ (*R*), −69.40 ppm (*S*).

 © 2009 Wiley-VCH Verlag GmbH & Co. KGaA, Weinheim

General procedure for analytical kinetic resolution: In the glove box, a screw cap NMR tube was charged with the catalyst (20 μmol), [D_6]benzene (0.5 mL), the substrate (1.00 mmol), and ferrocene (2 μmol) as the internal standard. The NMR tube was heated in a thermostat-controlled oil bath where required. The conversion was then monitored by NMR spectroscopy and the reactions were stopped after an appropriate conversion had been reached. Separation of the product pyrrolidine and the aminoalkene was achieved by aqueous extraction of the secondary ammonium acetate from the primary amine benzaldimine.[11c,d]

General procedure for preparative-scale kinetic resolution: In the glove box, a flask was charged with the catalyst (0.1 mmol), C_6H_6 (10 mL), and substrate (15.00 mmol). The conversion and enantiomeric excess of the starting material was then monitored by NMR spectroscopy and the reactions were stopped after a minimum of 98% *ee* had been reached. After a standard benzaldimine workup procedure,[11c,d] chiral amines were purified by vacuum distillation from CaH_2.

*[D_2]-(1S)-1-Phenylpent-4-en-1-amine ([D_2]**3a**)*: Prepared from (1*S*)-**3a** in an analogous procedure to that used to prepare racemic ([D_2]**3a**). Compound (1*S*)-**3a** was resolved from **3a** by using (*R*)-**1**–Lu as described previously.[11d]

*(1S)-1-(4-Methoxyphenyl)-pent-4-en-1-amine ((S)-**3b**)*: Compound (*S*)-**3b** was resolved from **3b** by (*R*)-**1**–Y (*f*=18), as a colorless liquid in 36% yield, b.p. 105 °C at 0.2 mmHg. Spectroscopic properties are in agreement with literature data.[11d]

*(1S)-1-(4-Chlorophenyl)-pent-4-en-1-amine ((S)-**3c**)*: Compound (*S*)-**3c** was resolved from **3c** by (*R*)-**2**–Y (*f*=19), as a colorless liquid in 30% yield, b.p. 100–110 °C at 0.2 mmHg. Spectroscopic properties are in agreement with literature data.[11d]

*(2S)-1-Phenylhex-5-en-2-amine ((S)-**3d**)*: Compound (*S*)-**3d** was resolved from **3d** by (*R*)-**1**–Y (*f*=5), as a colorless liquid in 12% yield, b.p. 103 °C at 0.2 mmHg. Spectroscopic properties are in agreement with literature data.[11d]

*(2R)-Hex-5-en-2-amine ((R)-**3e**)*: Compound (*R*)-**3e** was resolved from **3e** by (*R*)-**2**–Y (*f*=15), as a colorless liquid in 30% yield, b.p. 114 °C at 760 mmHg. $[\alpha]_D^{20}=-5.6$ (*c*=0.5 in MeOH). Spectroscopic properties are in agreement with literature data.[7i]

*(1S)-1-(Cyclohexyl)-hex-5-en-1-amine ((S)-**3f**)*: Compound (*S*)-**3f** was resolved from **3f** by (*R*)-**1**–Lu (*f*=6), as a colorless liquid in 9% yield, b.p. 80 °C at 0.2 mmHg. Spectroscopic properties are identical to those of racemic **3f**.

(1*R*)-1-(Methoxymethyl)pent-4-enylamine ((*R*)-3g):[17] A hot solution of **3g** (3.48 g, 27 mmol) and (*R*)-(−)-mandelic acid (4.12 g, 34 mmol) in isopropyl alcohol (40 mL) was allowed to cool slowly to 0 °C. The precipitated salt was filtered off after 12 h, dried in air, and recrystallized again. After 12 recrystallizations, more than 92% *ee* was achieved, according to ^{19}F NMR spectroscopy of the Mosher amide. The salt was treated with 10% aqueous NaOH (20 mL) and the amine was extracted with diethyl ether (2×40 mL). The combined extracts were dried over KOH and the diethyl ether was evaporated. The residue was distilled twice from CaH_2 under reduced pressure to give (*R*)-**3g** as a colorless liquid (0.45 g, 12%), b.p. 94–102 °C at 200 mmHg. Spectroscopic properties are identical to those of racemic **3g**.

(2*S*)-2-Phenyl-pent-4-en-1-amine ((*S*)-5): A hot solution of racemic **5** (5.44 g, 34 mmol) and (*R*)-(−)-mandelic acid (5.19 g, 34 mmol) in ethanol (40 mL) was allowed to cool slowly to 0 °C. The precipitated salt was filtered off, dried in air, and recrystallized again. After 13 recrystallizations, ≥98% *ee* was reached according to ^{19}F NMR spectroscopy of the Mosher amide. The salt was treated with 20% aqueous NaOH (20 mL) and the amine was extracted with Et_2O (2×40 mL). The combined extracts were dried over KOH and the diethyl ether was evaporated in vacuo. The resulting residue was distilled twice from CaH_2 under reduced pressure (b.p. 102 °C at 0.1 mmHg) to give (*S*)-**5** as a colorless liquid (0.75 g, 13%). Spectroscopic data are in agreement with the data reported in the literature.[7i]

Acknowledgements

Partial financial support of this research by the Deutsche Forschungsgemeinschaft (DFG) is gratefully acknowledged. The authors thank Prof. Daniel Seidel and Eric Klauber for their kind assistance with obtaining HPLC data.

[1] a) A. Ricci, *Modern Amination Methods*, Wiley-VCH, Weinheim, **2000**; b) A. Ricci, *Amino Group Chemistry: From Synthesis to the Life Sciences*, Wiley-VCH, Weinheim, **2008**.

[2] For general reviews on hydroamination, see: a) R. Taube in *Applied Homogeneous Catalysis, Vol. 1*, 1st ed. (Eds.: B. Cornils, W. A. Herrmann), VCH, Weinheim, **1996**, p. 507; b) T. E. Müller, M. Beller, *Chem. Rev.* **1998**, *98*, 675; c) T. E. Müller, M. Beller, *Transition Metals for Organic Synthesis, Vol. 2* (Eds.: M. Beller, C. Bolm), Wiley-VCH, Weinheim, **1998**, p. 316; d) J. J. Brunet, D. Neibecker in *Catalytic Heterofunctionalization from Hydroamination to Hydrozirconation* (Eds.: A. Togni, H. Grützmacher), Wiley-VCH, Weinheim, **2001**, p. 91; e) M. Nobis, B. Drießen-Hölscher, *Angew. Chem.* **2001**, *113*, 4105; *Angew. Chem. Int. Ed.* **2001**, *40*, 3983; f) J. Seayad, A. Tillack, C. G. Hartung, M. Beller, *Adv. Synth. Catal.* **2002**, *344*, 795; g) M. Beller, C. Breindl, M. Eichberger, C. G. Hartung, J. Seayad, O. R. Thiel, A. Tillack, H. Trauthwein, *Synlett* **2002**, 1579; h) J. F. Hartwig, *Pure Appl. Chem.* **2004**, *76*, 507; i) F. Pohlki, S. Doye, *Chem. Soc. Rev.* **2003**, *32*, 104; j) I. Bytschkov, S. Doye, *Eur. J. Org. Chem.* **2003**, 935; k) S. Doye, *Synlett* **2004**, 1653; l) S. Hong, T. J. Marks, *Acc. Chem. Res.* **2004**, *37*, 673; m) A. L. Odom, *Dalton Trans.* **2005**, 225; n) R. Severin, S. Doye, *Chem. Soc. Rev.* **2007**, *36*, 1407; o) T. E. Müller, K. C. Hultzsch, M. Yus, F. Foubelo, M. Tada, *Chem. Rev.* **2008**, *108*, 3795.

[3] a) P. W. Roesky, T. E. Müller, *Angew. Chem.* **2003**, *115*, 2812; *Angew. Chem. Int. Ed.* **2003**, *42*, 2708; b) K. C. Hultzsch, *Adv. Synth. Catal.* **2005**, *347*, 367; c) K. C. Hultzsch, *Org. Biomol. Chem.* **2005**, *3*, 1819; d) K. C. Hultzsch, D. V. Gribkov, F. Hampel, *J. Organomet. Chem.* **2005**, *690*, 4441; e) I. Aillaud, J. Collin, J. Hannedouche, E. Schulz, *Dalton Trans.* **2007**, 5105; f) G. Zi, *Dalton Trans.* **2009**, DOI: 10.1039/b906588a; g) A. L. Reznichenko, K. C. Hultzsch in *Chiral Amine Synthesis* (Ed.: T. Nugent), Wiley-VCH, Weinheim, in press.

[4] Sequential alkyne hydroamination–asymmetric hydrosilylation (or asymmetric transfer hydrogenation) represents an alternative to asymmetric hydroamination, see: a) A. Heutling, F. Pohlki, I. Bytschkov, S. Doye, *Angew. Chem.* **2005**, *117*, 3011; *Angew. Chem. Int. Ed.* **2005**, *44*, 2951; b) X.-Y. Liu, C.-M. Che, *Org. Lett.* **2009**, *11*, 4204.

[5] For some recent examples, see: a) A. Tillack, V. Khedkar, H. Jiao, M. Beller, *Eur. J. Org. Chem.* **2005**, 5001; b) J. Takaya, J. F. Hartwig, *J. Am. Chem. Soc.* **2005**, *127*, 5756; c) C. S. Yi, S. Y. Yun, I. A. Guzei, *J. Am. Chem. Soc.* **2005**, *127*, 5782; d) J.-J. Brunet, N. C. Chu, O. Diallo, *Organometallics* **2005**, *24*, 3104; e) A. M. Johns, M. Utsunomiya, C. D. Incarvito, J. F. Hartwig, *J. Am. Chem. Soc.* **2006**, *128*, 1828; f) O. Jimenez, T. E. Müller, C. Siever, A. Spirkl, J. A. Lercher, *Chem. Commun.* **2006**, 2974; g) R. L. LaLonde, B. D. Sherry, E. J. Kang, F. D. Toste, *J. Am. Chem. Soc.* **2007**, *129*, 2452; h) J. Zhou, J. F. Hartwig, *J. Am. Chem. Soc.* **2008**, *130*, 12220; i) Z. Zhang, S. D. Lee, R. A. Widenhoefer, *J. Am. Chem. Soc.* **2009**, *131*, 5372.

[6] For hydroamination catalyzed by cyclopentadienyl rare-earth-metal complexes, see: a) M. R. Gagné, C. L. Stern, T. J. Marks, *J. Am. Chem. Soc.* **1992**, *114*, 275; b) Y. Li, T. J. Marks, *J. Am. Chem. Soc.* **1996**, *118*, 9295; c) Y. Li, T. J. Marks, *J. Am. Chem. Soc.* **1998**, *120*, 1757; d) A. T. Gilbert, B. L. Davis, T. J. Emge, R. D. Broene, *Organometallics* **1999**, *18*, 2125; e) V. M. Arredondo, S. Tian, F. E. McDonald, T. J. Marks, *J. Am. Chem. Soc.* **1999**, *121*, 3633; f) G. A. Molander, E. D. Dowdy, *J. Org. Chem.* **1999**, *64*, 6515; g) V. M. Arredondo, F. E. McDonald, T. J. Marks, *Organometallics* **1999**, *18*, 1949; h) G. A. Molander, E. D. Dowdy, S. K. Pack, *J. Org. Chem.* **2001**, *66*, 4344; i) G. A. Molander, S. K. Pack, *Tetrahedron* **2003**, *59*, 10581; j) G. A. Molander, S. K. Pack, *J. Org. Chem.* **2003**, *68*, 9214; k) J.-S. Ryu, G. Y. Li, T. J. Marks, *J. Am. Chem. Soc.* **2003**, *125*, 12584; l) J.

 © 2009 Wiley-VCH Verlag GmbH & Co. KGaA, Weinheim

Zhao, T. J. Marks, *Organometallics* **2006**, *25*, 4763; m) S. B. Amin, S. Y. Seo, T. J. Marks, *Organometallics* **2008**, *27*, 2411; n) H. F. Yuen, T. J. Marks, *Organometallics* **2009**, *28*, 2423.

[7] For achiral, non-metallocene, rare-earth-metal-based hydroamination catalysts, see: a) M. R. Bürgstein, H. Berberich, P. W. Roesky, *Organometallics* **1998**, *17*, 1452; b) M. R. Bürgstein, H. Berberich, P. W. Roesky, *Chem. Eur. J.* **2001**, *7*, 3078; c) Y. K. Kim, T. Livinghouse, J. E. Bercaw, *Tetrahedron Lett.* **2001**, *42*, 2933; d) Y. K. Kim, T. Livinghouse, *Angew. Chem.* **2002**, *114*, 3797; *Angew. Chem. Int. Ed.* **2002**, *41*, 3645; e) Y. K. Kim, T. Livinghouse, Y. Horino, *J. Am. Chem. Soc.* **2003**, *125*, 9560; f) F. Lauterwasser, P. G. Hayes, S. Bräse, W. E. Piers, L. L. Schafer, *Organometallics* **2004**, *23*, 2234; g) K. C. Hultzsch, F. Hampel, T. Wagner, *Organometallics* **2004**, *23*, 2601; h) T. K. Panda, A. Zulys, M. T. Gamer, P. W. Roesky, *Organometallics* **2005**, *24*, 2197; i) J. Y. Kim, T. Livinghouse, *Org. Lett.* **2005**, *7*, 4391; j) S. Bambirra, H. Tsurugi, D. van Leusen, B. Hessen, *Dalton Trans.* **2006**, 1157; k) H. Kim, T. Livinghouse, J. H. Shim, S. G. Lee, P. H. Lee, *Adv. Synth. Catal.* **2006**, *348*, 701; l) M. Rastätter, A. Zulys, P. W. Roesky, *Chem. Eur. J.* **2007**, *13*, 3606; m) E. Lu, W. Gan, Y. Chen, *Organometallics* **2009**, *28*, 2318.

[8] For catalyst systems for the hydroamination of aminoalkenes based on metals other than rare-earth metals, see: a) A. Ates, C. Quinet, *Eur. J. Org. Chem.* **2003**, 1623; b) P. D. Knight, I. Munslow, P. N. O'Shaughnessy, P. Scott, *Chem. Commun.* **2004**, 894; c) D. V. Gribkov, K. C. Hultzsch, *Angew. Chem.* **2004**, *116*, 5659; *Angew. Chem. Int. Ed.* **2004**, *43*, 5542; d) J. A. Bexrud, J. D. Beard, D. C. Leitch, L. L. Schafer, *Org. Lett.* **2005**, *7*, 1959; e) C. F. Bender, R. A. Widenhoefer, *J. Am. Chem. Soc.* **2005**, *127*, 1070; f) M. R. Crimmin, I. J. Casely, M. S. Hill, *J. Am. Chem. Soc.* **2005**, *127*, 2042; g) H. Kim, P. H. Lee, T. Livinghouse, *Chem. Commun.* **2005**, 5205; h) N. Meyer, K. Löhnwitz, A. Zulys, P. W. Roesky, M. Dochnahl, S. Blechert, *Organometallics* **2006**, *25*, 3779; i) R. K. Thomson, J. A. Bexrud, L. L. Schafer, *Organometallics* **2006**, *25*, 4069; j) D. A. Watson, M. Chiu, R. G. Bergman, *Organometallics* **2006**, *25*, 4731; k) P. Horrillo-Martínez, K. C. Hultzsch, F. Hampel, *Chem. Commun.* **2006**, 2221; l) M. C. Wood, D. C. Leitch, C. S. Yeung, J. A. Kozak, L. L. Schafer, *Angew. Chem.* **2007**, *119*, 358; *Angew. Chem. Int. Ed.* **2007**, *46*, 354; m) A. L. Gott, A. J. Clarke, G. J. Clarkson, P. Scott, *Organometallics* **2007**, *26*, 1729; n) B. D. Stubbert, T. J. Marks, *J. Am. Chem. Soc.* **2007**, *129*, 4253; o) B. D. Stubbert, T. J. Marks, *J. Am. Chem. Soc.* **2007**, *129*, 6149; p) T. Ogata, A. Ujihara, S. Tsuchida, T. Shimizu, A. Kaneshige, K. Tomioka, *Tetrahedron Lett.* **2007**, *48*, 6648; q) C. Liu, J. F. Hartwig, *J. Am. Chem. Soc.* **2008**, *130*, 1570; r) C. F. Bender, W. B. Hudson, R. A. Widenhoefer, *Organometallics* **2008**, *27*, 2356; s) C. Quinet, P. Jourdain, C. Hermans, A. Ates, I. Lucas, I. E. Markó, *Tetrahedron* **2008**, *64*, 107; t) A. L. Gott, A. J. Clarke, G. J. Clarkson, P. Scott, *Chem. Commun.* **2008**, 1422; u) A. L. Gott, G. J. Clarkson, R. J. Deeth, M. L. Hammond, C. Morton, P. Scott, *Dalton Trans.* **2008**, 2983; v) P. Horrillo-Martínez, K. C. Hultzsch, *Tetrahedron Lett.* **2009**, *50*, 2054; w) K. Löhnwitz, M. J. Molski, A. Lühl, P. W. Roesky, M. Dochnahl, S. Blechert, *Eur. J. Inorg. Chem.* **2009**, 1369; x) M. R. Crimmin, M. Arrowsmith, A. G. M. Barrett, I. J. Casely, M. S. Hill, P. A. Procopiou, *J. Am. Chem. Soc.* **2009**, *131*, 9670.

[9] For asymmetric hydroamination catalyzed by cyclopentadienyl rare-earth-metal complexes, see: a) M. A. Giardello, V. P. Conticello, L. Brard, M. R. Gagné, T. J. Marks, *J. Am. Chem. Soc.* **1994**, *116*, 10241; b) M. R. Douglass, M. Ogasawara, S. Hong, M. V. Metz, T. J. Marks, *Organometallics* **2002**, *21*, 283; c) S. Hong, A. M. Kawaoka, T. J. Marks, *J. Am. Chem. Soc.* **2003**, *125*, 15878; d) J.-S. Ryu, T. J. Marks, F. E. McDonald, *J. Org. Chem.* **2004**, *69*, 1038; e) D. V. Vitanova, F. Hampel, K. C. Hultzsch, *J. Organomet. Chem.* **2007**, *692*, 4690.

[10] a) P. N. O'Shaughnessy, P. D. Knight, C. Morton, K. M. Gillespie, P. Scott, *Chem. Commun.* **2003**, 1770; b) P. N. O'Shaughnessy, P. Scott, *Tetrahedron: Asymmetry* **2003**, *14*, 1979; c) S. Hong, S. Tian, M. V. Metz, T. J. Marks, *J. Am. Chem. Soc.* **2003**, *125*, 14768; d) J. Collin, J.-D. Daran, E. Schulz, A. Trifonov, *Chem. Commun.* **2003**, 3048; e) P. N. O'Shaughnessy, K. M. Gillespie, P. D. Knight, I. Munslow, P. Scott, *Dalton Trans.* **2004**, 2251; f) J. Y. Kim, T. Livinghouse, *Org. Lett.* **2005**, *7*, 1737; g) J. Collin, J.-D. Daran, O. Jacquet, E. Schulz, A. Trifonov, *Chem. Eur. J.* **2005**, *11*, 3455; h) D. Riegert, J. Collin, A. Meddour, E. Schulz, A. Trifonov, *J. Org. Chem.* **2006**, *71*, 2514; i) N. Meyer, A. Zulys, P. W. Roesky, *Organometallics* **2006**, *25*, 4179; j) H. Kim, Y. K. Kim, J. H. Shim, M. Kim, M. Han, T. Livinghouse, P. H. Lee, *Adv. Synth. Catal.* **2006**, *348*, 2609; k) X. Yu, T. J. Marks, *Organometallics* **2007**, *26*, 365; l) R. Heck, E. Schulz, J. Collin, J.-F. Carpentier, *J. Mol. Catal. A* **2007**, *268*, 163; m) D. Riegert, J. Collin, J.-D. Daran, T. Fillebeen, E. Schulz, D. Lyubov, G. Fukin, A. Trifonov, *Eur. J. Inorg. Chem.* **2007**, 1159; n) L. Xiang, Q. Wang, H. Song, G. Zi, *Organometallics* **2007**, *26*, 5323; o) J. Hannedouche, I. Aillaud, J. Collin, E. Schulz, A. Trifonov, *Chem. Commun.* **2008**, 3552; p) G. Zi, L. Xiang, H. Song, *Organometallics* **2008**, *27*, 1242; q) I. Aillaud, D. Lyubov, J. Collin, R. Guillot, J. Hannedouche, E. Schulz, A. Trifonov, *Organometallics* **2008**, *27*, 5929; r) Q. Wang, L. Xiang, H. Song, G. Zi, *Inorg. Chem.* **2008**, *47*, 4319.

[11] a) D. V. Gribkov, K. C. Hultzsch, F. Hampel, *Chem. Eur. J.* **2003**, *9*, 4796; b) D. V. Gribkov, F. Hampel, K. C. Hultzsch, *Eur. J. Inorg. Chem.* **2004**, 4091; c) D. V. Gribkov, K. C. Hultzsch, *Chem. Commun.* **2004**, 730; d) D. V. Gribkov, K. C. Hultzsch, F. Hampel, *J. Am. Chem. Soc.* **2006**, *128*, 3748.

[12] For general reviews on the application of chiral rare-earth-metal catalysts in organic synthesis, see: a) K. Mikami, M. Terada, H. Matsuzawa, *Angew. Chem.* **2002**, *114*, 3704; *Angew. Chem. Int. Ed.* **2002**, *41*, 3554; b) H. C. Aspinall, *Chem. Rev.* **2002**, *102*, 1807; c) M. Shibasaki, N. Yoshikawa, *Chem. Rev.* **2002**, *102*, 2187; d) S. Kobayashi, M. Sugiura, H. Kitagawa, W. W.-L. Lam, *Chem. Rev.* **2002**, *102*, 2227.

[13] For general reviews on the chemistry of cyclopentadienyl-free rare-earth-metal complexes, see: a) F. T. Edelmann, *Angew. Chem.* **1995**, *107*, 2647; *Angew. Chem. Int. Ed. Engl.* **1995**, *34*, 2466; b) F. T. Edelmann, D. M. M. Freckmann, H. Schumann, *Chem. Rev.* **2002**, *102*, 1851; c) W. E. Piers, D. J. H. Emslie, *Coord. Chem. Rev.* **2002**, *233–234*, 131.

[14] For the gold-catalyzed dynamic kinetic resolution of aminoallenes through hydroamination–cyclization, see: Z. Zhang, C. F. Bender, R. A. Widenhoefer, *J. Am. Chem. Soc.* **2007**, *129*, 14148.

[15] The (dynamic) kinetic resolution of racemic amines can be effected by using various enzymatic methodologies; for selected examples, see: a) F. van Rantwijk, R. A. Sheldon, *Tetrahedron* **2004**, *60*, 501; b) C. J. Dunsmore, R. Carr, T. Fleming, N. J. Turner, *J. Am. Chem. Soc.* **2006**, *128*, 2224; c) A. N. Parvulescu, P. A. Jacobs, D. E. De Vos, *Chem. Eur. J.* **2007**, *13*, 2034; d) C. E. Hoben, L. Kanupp, J.-E. Bäckvall, *Tetrahedron Lett.* **2008**, *49*, 977; e) A. N. Parvulescu, P. A. Jacobs, D. E. De Vos, *Adv. Synth. Catal.* **2008**, *350*, 113; f) H. Ismail, R. M. Lau, F. van Rantwijk, R. A. Sheldon, *Adv. Synth. Catal.* **2008**, *350*, 1511; g) M. D. Truppo, N. J. Turner, J. D. Rozzell, *Chem. Commun.* **2009**, 2127.

[16] For the sake of simplicity k_R/k_S represents k_{fast}/k_{slow} for all substrates. Note, however, that for substrate **3e** the *S* enantiomer is the faster reacting enantiomer when using the (*R*)-binaphtholate catalysts.

[17] A preliminary X-ray crystallographic analysis of the ammonium salt of (*R*)-**3g** with (*R*)-(−)-mandelic acid confirmed the assigned absolute configuration relative to the known configuration of mandelic acid. Also, the ^{19}F NMR spectroscopic chemical shift of the Mosher amide of **3g** obtained in the fractional crystallization is in agreement with this assignment.

[18] M. N. Bochkarev, *Chem. Rev.* **2002**, *102*, 2089.

[19] CCDC-739753 contains the supplementary crystallographic data for the (*R*)-Mosher amide of (*S*)-**5**. These data can be obtained free of charge from The Cambridge Crystallographic Data Centre via www.ccdc.cam.ac.uk/data_request/cif.

[20] Q. Yang, J. E. Ney, J. P. Wolfe, *Org. Lett.* **2005**, *7*, 2575.

[21] P. M. Smith, E. J. Thomas, *J. Chem. Soc. Perkin Trans. 1* **1998**, 3541.

[22] M. Gao, D.-X. Wang, Q.-Y. Zheng, M.-X. Wang, *J. Org. Chem.* **2006**, *71*, 9532.

Received: August 11, 2009
Published online: October 15, 2009

 © 2009 Wiley-VCH Verlag GmbH & Co. KGaA, Weinheim